Therapeutic Targeting of Histone Lysine Demethylase KDM4B Blocks the Growth of Castration-resistant Prostate Cancer

Lingling Duan
UT Southwestern: The University of Texas Southwestern Medical Center
Yu-An Chen
UT Southwestern: The University of Texas Southwestern Medical Center
Yanping Liang
Sun Yat-sen University
Zhenhua Chen
Sun yat-sen university
Jun Lu
sun yat-sen university
Yong Fang
Sun Yat-Sen University
Jiazheng Cao
sun-yat-sen university
Jian Lu
Jiangmen Hospital, Sun Yat-Sen University
Hongwei Zhao
Qindao University Medical College Affiliated Yantai Yuhuangding Hospital
Rey-Chen Pong
UT Southwestern: The University of Texas Southwestern Medical Center
Elizabeth Hernandez
UT Southwestern: The University of Texas Southwestern Medical Center
Payal Kapur
UT Southwestern: The University of Texas Southwestern Medical Center
Tram Anh T Tran
UT Southwestern: The University of Texas Southwestern Medical Center
Tristan Smith
University of Texas at Dallas
Elisabeth D. Martinez
UT Southwestern: The University of Texas Southwestern Medical Center
Jung-mo Ahn

University of Texas at Dallas

Jer-Tsong Hsieh

UT Southwestern: The University of Texas Southwestern Medical Center

Junhang Luo

first affiliated hospital of sun yat-sen university

Zhi-Ping Liu (zhi-ping.liu@utsouthwestern.edu)

UT Southwestern: The University of Texas Southwestern Medical Center https://orcid.org/0000-0003-1341-3878

Research

Keywords: histone lysine demethylase, KDM4B, KDM inhibitor, castration-resistant prostate cancer, prostate therapy

Posted Date: October 11th, 2021

DOI: https://doi.org/10.21203/rs.3.rs-957516/v1

Abstract

Background: Accumulating evidence points to epigenetic mechanisms as essential in tumorigenesis. Treatment that targets epigenetic regulators is becoming an attractive strategy for cancer therapy. The role of epigenetic therapy in prostate cancer (PCa) remains elusive. Previously we demonstrated a correlation of levels of histone lysine demethylase KDM4B with the appearance of castration resistant prostate cancer (CRPC) and identified a small molecular inhibitor of KDM4B, B3. In this study, we aim to define the role of KDM4B in promoting PCa progression and test the efficacy of B3 using clinically relevant PCa models.

Methods: KDM4B was overexpressed in LNCaP cells or knocked down (KD) in 22Rv1 cells. The specificity of B3 was determined in vitro using recombinant KDM proteins and in vivo using 22Rv1 cell lysates. The efficacy of B3 monotherapy or in combination with androgen receptor (AR) antagonist enzalutamide or the mTOR inhibitor rapamycin was tested using xenograft models in castrated mice. Comparative transcriptomic analysis was performed on KDM4B KD and B3-treated 22Rv1 cells to determine the on-target (KDM4B-dependent) and off-target (non-KDM4B-associated) effects of B3.

Results: Overexpression of KDM4B in LNCaP cells enhanced its tumorigenicity whereas knockdown of KDM4B in 22Rv1 cells reduced tumor growth in castrated mice. B3 suppressed the growth of both 22Rv1 and VCaP xenografts and sensitized 22Rv1 cells to enzalutamide inhibition. B3 also inhibited 22Rv1 tumor growth synergistically with rapamycin that resulted in cell apoptosis. Mechanistically, B3 inhibited expression of AR-V7 and genes involved in epithelial-to-mesenchymal transition. DNA replication stress marker γH2A.X was upregulated by B3, which is further increased when combined with rapamycin. Based on transcriptomic and biochemical analyses, B3 inhibits both H3K9me3 and H3K27me3 demethylase activity, which is believed to underlie its anti-tumor action.

Conclusions: Our studies establish KDM4B as a potent target for CRPC and B3 as a potential therapeutic agent. B3 as monotherapy or in combination with other anti-PCa therapeutics offers proof of principle for the clinical translation of epigenetic therapy targeting KDMSs for CRPC patients.

Background

Prostate cancer (PCa) is the second most commonly diagnosed cancer and the second leading cause of cancer death among US men, with an estimated 248,530 new cancer cases and 34,130 deaths in 2021 (1). Although mortality of PCa is decreasing due to the effective local therapies for men diagnosed with organ-confined disease, the overall survival for patients with castration resistant prostate cancer (CRPC) remains poor. Moreover, therapy resistant CRPC (t-CRPC) is considered an end disease when the tumor acquires resistant to first and second-generation of Androgen Receptor Pathway Inhibitors (ARPIs). In general, the mechanism underlying t-CRPC remains elusive because it is highly heterogeneous and complex. Nevertheless, several mechanisms are emerging including the appearance of constitutively active AR variants (AR-Vs) such as AR-V7 that lack the canonical ligand-binding domain (2–10) and

treatment-related lineage switch from epithelial to neuroendocrine, which gives rise to AR-negative CRPC with neuroendocrine cell-like features (NEPC) (11, 12). NEPC accounts for approximately 25% of lethal PCa diagnosed per year in the United States (13). As the AR signaling remains a pivotal driver for the disease progression despite castration levels of androgen, the prevalence of t-CRPC and NEPC is expected to rise due to the earlier usage of more potent anti-androgen agents. Thus, new agents different from targeting AR-signaling are highly desired.

Epigenetics is an emerging mechanism for tumorigenesis (14). Post-translational modification of histone including histone methylation affects chromatic structures and can determine transcriptional outcome. KDM4B/JMJD2B is a member of the Jumonji C (JmjC)-domain containing histone lysine demethylase 4 (KDM4) family (15). KDM4B demethylates H3K9me3 (16), a heterochromatin mark associated with a closed chromatin structure and inhibition of gene transcription. KDM4B is upregulated in a variety of human cancers (17, 18). Overexpression of KDM4B has been shown to promote the growth of breast, gastric, colorectal, and liver cancer (19–21). KDM4B is part of DNA damage response complex and promotes cell survival following irradiation (22). KDM4B may be associated with an aggressive subtype of classical Hodgkin lymphoma and radiation resistance (23). KDM4B promotes epithelial-to-mesenchymal transition (EMT) leading to pancreatic cancer metastases (24). KDM4B is highly expressed in *MYCN*-amplified neuroblastomas with poor outcome (25). Our previous studies showed that KDM4B is also upregulated in PCa (26, 27). KDM4B is a known co-activator of AR (17). We have shown that KDM4B also has AR-independent functions in PCa, activating cell cycle gene expression such as PLK1 and promoting cell cycle progression as a co-activator of BMYB (27). Most recently, we found that KDM4B can promote AR-V7 expression via regulating the alternative splicing of AR (28). KDM4B can be phosphorylation by protein kinase A (PKA) under conditions that promote castration-resistance, eliciting its binding to general splicing factor SF3B3. KDM4B opens up the chromatin around the alternative exon by removing the heterochromatin mark H3K9me3. Moreover, KDM4B binds specific RNA sequence near the 5’-crptic exon 3 (CE3). As a result of these interactions, KDM4B can recruit and stabilize the spliceosome near the cryptic exon, promoting its inclusion. These studies suggest that KDM4B promotes prostate tumorigenesis via at least three mechanisms; 1) as an AR-co-activator in the AR-signaling pathway under hormone-sensitive conditions, 2) promoting cell cycle progression as a BMYB-coactivator in the absence of the AR-signaling such as in NEPC, and 3) promoting CRPC via alternative splicing of AR-V7 in response to castration in AR-positive cells, and implicate that targeting KDM4B may be therapeutic effective in broad range of PCa pathologies including both AR-dependent and AR-independent PCa.

In this study, we provide further supporting evidence for the aforementioned hypothesis. Previously we identified several KDM4 inhibitors including B3 from the NIH chemical library and showed its inhibitory effect on NEPC- PC3 xenograft *in vivo* (27). Here, we evaluate the efficacy of B3 monotherapy or in combination with other targeted therapeutics using clinically relevant t-CRPC models. We show that inactivation of KDM4B genetically or pharmacologically inhibited 22Rv1 tumor growth in castrated mice. B3 can sensitize 22Rv1 cells to enzalutamide inhibition as well as synergize with the mTOR pathway inhibitor rapamycin. Mechanistically, the synergistic effect of B3 with enzalutamide or rapamycin may

arise from their suppression of AR/AR-V7 signaling and induction of DNA replication stress, respectively. Our studies establish KDM4B as a potent target for t-CRPC and suggest the potential clinical utility of KDM4 inhibitor B3 as a mono or combination therapy in CRPC.

Materials And Methods

Plasmids, cell culture, transfection, stable cell line, and minigene reporter assays

KDM4B plasmids were described previously (27). human PCa cell line LNCaP, VCaP, and 22Rv1 were purchased from ATCC (Manassas VA, USA) and routinely authenticated using method described in the original paper and/or the short tandem repeat (STR) DNA profiling technology by the Genomic Core facility of UT Southwestern. Cells were cultured in RPMI1640 medium supplemented with FBS or charcoal stripped FBS (CFBS) (Highclone, Logan UT, USA) as indicated. Stable cell lines LNCaP-ctl and LNCaP-4B were established using lentiviruses expressing vector and Flag-KDM4B, respectively, and subsequent selection with blasticidin. Plasmids and siRNA transfections were performed using lipofectamine 3000 and RNAimax, respectively.

Targeted deletion of KDM4B with CRISPR/CAS9

22Rv1 cells were electroporated with U6 target gRNA expression vector containing KDM4B-targeted gRNA (GCTGCAGCCATGGGGTCTCAGG) or lentiCRISP-GFP-v2 containing non-targeted control gRNA (CGCTTCCGCGGCCCGTTCA) along with plasmid expressing CAS9 (29). Cells were FACS sorted in single cell to 96-well plates. Clonal cells were genotyped. Deletion or KD of KDM4B was confirmed by qPR-PCR and western blot analysis. Multiple clonal controls were selected and showed no difference in growth rate.

Cell proliferation assays

Cell proliferation assays were performed using MTT cell proliferation assay kit (ATCC) or trypan blue staining. For drug inhibition assay, cells were seeded for one day before various concentrations of drug were added. Cells were cultured for additional 3 days before harvested for MTT/trypan blue assays.

RNA isolation, quantitative real-time polymerase chain reaction (qRT-PCR), and RNA-seq

Total RNA was isolated using TRIzol reagent (Invitrogen) according to manufacturer's procedures. RNA (5 µg) was used to generate cDNA using Superscript III (Invitrogen). qRT-PCR was performed using SYBR Green (BioRad) with gene-specific primers. Data were normalized to an internal standard as indicated (ΔC_T method). RNA-seq experiments were performed commercially by Novogene. qRT-PCR primers were listed in supplemental table 1.

Antibodies, immunoblotting, immunoprecipitation, and immunofluorescence

Following antibodies were used: pmTOR, mTOR, pS6, S6 kinase, KDM4B, Histone 3, cleaved PARP1, KDM6A, and KDM6B (Cell signaling), H3K9me3 and H3K27me3 (Abcam), GAPDH and SNAI2 (Santa

Cruz), E-cadherin (BD company), SYP, PSA, and AR (cell Margue), and AR-V7 (Proteintech). Immunoblotting, immunoprecipitation, and immunofluorescence were performed according to the standard protocol.

IHC and scoring

Histological sections of prostate biopsy tissue samples from 106 patients with localized or metastatic hormone-sensitive prostate cancer (AJCC stage III and IV) underwent ADT (supplemental Table S2) were stained with anti-KDM4B antibody. These patients with informed consent were from the First Affiliated Hospital of Sun Yat-sen University, Jiangmen Hospital of Sun Yat-sen University and Affiliated Yantai Yuhuangding Hospital of Qingdao University Medical College from January 2000 to December 2010. Slides were examined and scored by two experienced pathologists independently who were blind to all clinical data. KDM4B expression was evaluated considering only the carcinoma cells and using a semi-quantitative scoring system. Briefly, the number of positive cells were counted and scaled: 0, no positive cells; 1, 1-25% positive cells; 2, 26-50% positive cells; 3, 51-75% positive cells; 4, 76-100% positive cells. 0-2 was regarded as low expression group and 3-4 was high expression group. We then analyzed the effect of KDM4B expression on patients' overall survival time via Kaplan-Meier survival analysis and COX Proportional Hazard Model.

Xenograft model

PCa cells ($3x10^6$ cells/site) mixed with Matrigel (BD Biosciences) were injected subcutaneously into right and left leg of NOD/SCID mouse. Once tumor becomes palpable, tumor volume (mm^3) was measured every 3 days with caliper and was calculated using the ellipsoid formula ($\pi/6$ x length x width x depth). For drug treatment, mice bearing palpable xenografts were randomized into different groups treated with vehicles, B3, enzalutamide, rapamycin, B3+enzalutamide, B3+rapamycin. Drugs were administered using minipump continuously for 7 days (for VCaP xenograft) or intraperitoneal injection with 3 times/weeks for 2 weeks at dose indicated in the respective figures (For 22Rv1 xenograft). Tumors were excised and weighted at time of sacrifice and used for target validation. All animal protocols were approved by the Institutional Animal Care and Use Committee in UT Southwestern Medical Center. Only male mice were used since prostate cancer is male-only disease.

Ex vivo culture of human prostate tumors

Fresh prostate tumor was obtained with informed consent from a 68 years-old man with Gleason 9 metastatic PCa undergoing radical prostatectomy at the first affiliated hospital of Sun-Yat-San university. The patient was previously diagnosed with Gleason 8 (5+3) PCa, gave up the surgery voluntarily, and chose bicalutamide 50mg once daily. After 20 months anti-androgen therapy, PCa progressed to Gleason 9 (5+4) and can be considered as CRPC. Tissues were cultured at 37^oC with vehicle (DMSO) alone or B3 2.5 (μM) for two days as described (27), then formalin-fixed and paraffin-embedded for IHC.

Jumonji histone demethylase activity assays

Nuclear extracts were generated using cells treated with B3 or vehicle for 24 hours using EpiQuik Nuclear Extraction Kit (Epigentek, OP-0002-1) according to the manufacturer's instructions. Nuclear extracts were used as the enzyme source to measure demethylase activity on exogenous H3K4me3, H3K9me3 or H3K27me3 substrates, using Epigenase JARID Demethylase Activity/Inhibition Assay Kit (Epigentek, P-3083) for H3K4me3 demethylation, Epigenase™ JMJD2 Demethylase Activity/Inhibition Assay Kit (Epigentek, P-3081) for H3K9me3 demethylation and Epigenase™ JMJD3/UTX Demethylase Activity/Inhibition Assay Kit (Epigentek, P-3085) for H3K27me3 demethylation. The reaction was carried out in 50 µL reactions with 1 mM α-ketoglutarate, 2 mM ascorbate, 100 mM (NH4)2Fe(SO4)2.6H2O (Sigma, 215406), 50 ng substrate (either H3K4me3, H3K9me3 or H3K27me3), 0.25x of EDTA free protease inhibitor (Roche, 05 892 791 001) and 15 mg nuclear extract at 37^{o}C for 2 hours. A mix of nuclear extracts that were subjected to heat inactivation at 95^{o}C for 10 minutes then cooled to 30^{o}C was used as the negative control. Activity was determined by subtracting the values obtained from the heat inactive samples from the active nuclear extracts for reactions performed at the same time.

Statistical analysis

All data are shown as mean ± SD or SEM as stated. Student's *t* test (2-tailed) was used to compare the difference between 2 groups that passed normality test. $p < 0.05$ was considered statistically significant. Graphpad Prism 9 was used to calculate IC_{50}.

Results

KDM4B promotes prostate tumorigenesis

Previously we showed that overexpression of KDM4B in androgen responsive LNCaP cells promoted cell growth in vitro (26, 27). Whether KDM4B promotes castration-resistance remains unknown. KDM4B is upregulated in LNCaP cells under androgen-deprived (CFBS) or anchorage-independent (with methylcellulose) conditions (Fig. 1A). We established a stable LNCaP cells expressing Flag-tagged KDM4B (LNCaP-4B). Overexpression of KDM4B promoted the proliferation of LNCaP in both FBS and CFBS-containing medium (Fig. 1B). LNCaP-4B cells had significantly enhanced cell migration compared to control vector transfected LNCaP-ctl cells (Fig. 1C). To test the clinical relevance of KDM4B in PCa progression, we stained prostate biopsy tissue samples for KDM4B expression from patients with localized or metastatic hormone sensitive PCa (AJCC stage III and IV) who underwent androgen deprivation therapy. Significant KDM4B staining was observed in the tumor samples whereas little was found in the normal tissue (Fig. 1D). Patients with higher KDM4B expression had significantly shorter survival rate (Fig. 1E). We tested the effect of overexpression of KDM4B in vivo. A 30% tumor-take rate was observed in mice injected with LNCaP-4B cells whereas mice injected with control LNCaP-ctl cells showed no tumor (Fig. 1F). LNCaP-4B cells failed to form tumor in castrated animals (data not shown).

KDM4B knockdown inhibits CRPC growth

Previously we established stable clonal KDM4B knockdown (KD) 22Rv1 cell lines (cl4 and cl7) using CRISPR/Cas9 technology (Supplemental Figure 1) and showed that KDM4B KD reduced cell growth under both CFBS and FBS culture conditions compared to non-targeting control-transfected 22Rv1 cells (ctl) in either AR-V7 dependent (in CFBS) and independent (in FBS) manner, respectively (26). Expressional analysis with qRT-PCR showed that genes known to be regulated by AR-V7 such as END2, SNAI2, and TMPRSS2 are downregulated in KDM4B KD (cl4 and cl7) cells and can be rescued by re-expression of AR-V7 (Fig. 2A) whereas re-expression of AR-V7 in KDM4B KD cells has little effect on cell cycle genes that are regulated by KDM4B but not AR-V7 (Fig. 2B), further suggesting that KDM4B can regulate 22Rv1 cell growth via both AR-V7-dependent and AR-V7 independent pathway. AR-V7 is known to promote EMT that is associated with PCa aggressiveness (30). Immunofluorescence staining indicated that 22Rv1-ctl cells had intracellular E-cad staining whereas KDM4B KD cells had membrane E-cad staining (Fig. 2C), suggesting that inactivation of *KDM4B* resulted in a more epithelial-cell like phenotype. Re-expression of AR-V7 in KDM4B KD cells reversed the membrane staining of E-cad, suggesting KDM4B may promote EMT via AR-V7.

We tested the effect of KDM4B KD on the growth of t-CRPC tumor using 22Rv1 model. 22Rv1-cl4 and cl7-derived xenografts were significantly smaller than 22Rv1-ctl xenografts in castrated hosts (Fig. 2D). IHC staining (Fig. 2E) and immunoblotting (Fig. 2F) showed significantly reduced AR-V7 in KDM4B-KD tumors whereas AR-expression remained similar, suggesting the effect of KDM4B on tumor growth is related to AR-V7. SNAI2, an AR-V7-regulated and EMT-associated gene was also downregulated in KDM4B KD cl4 and cl7 cells. In addition, we noticed that the presence of SYP, a neuroendocrine marker, in 22Rv1-tumors was also abolished in KDM4B KD-tumors (Fig. 2G). Re-expression of exogenous AR-V7 in KDM4B-cl7 cells partially reversed the inhibitory effect of KDM4B KD on tumor growth (Fig. 2H). These data suggest that KDM4B is required for androgen-independent growth of 22Rv1 tumor, and its action is at least partially mediated by AR-V7.

Pharmacological inhibition of KDM4B suppresses CRPC tumor growth

To evaluate the efficacy of B3 on 22Rv1 tumor growth in vivo, B3 was injected intraperitoneally into castrated hosts 3 times/week for 2 weeks. B3 significantly suppressed the growth of 22Rv1 tumor in a dose-dependent manner (Fig. 3A-B). Target analysis by western blot and immunohistochemistry revealed that AR-V7 expression in B3-treated tumors was downregulated (Fig. 3C-D). B3 also inhibited VCaP tumor growth in vivo (Fig. 3E). We tested the effect of B3 on *ex vivo* human prostate tumors from a CRPC patient. Treatment of the ex vivo CRPC specimen with B3 effectively abolished tumor AR-V7 expression (Fig. 3F). Unlike KDM4B KD that did not alter the AR expression in tumor, B3 treatment at 50 mg/kg resulted in a significant downregulation of the AR expression, suggesting presence of off-target effect. The effect of B3 on AR is dose dependent as the AR expression remained similar in tumors treated with 10mg/kg compared to vehicle treated ones (Fig. 3G).

B3 sensitizes CRPC cells to enzalutamide treatment

22Rv1 cells are resistant to enzalutamide due to the presence of AR-V7. As B3 can inhibit AR-V7 expression, we reasoned that B3 may sensitize 22Rv1 cells to enzalutamide. Indeed, B3 sensitized the response of 22Rv1 cells to enzalutamide with estimated combination index (CI) of 0.46 (Fig. 4A-B). The combination therapy also resulted in more significant inhibition of 22Rv1 xenograft growth than single agent alone in vivo (Fig. 4C-F), suggesting a synergistic effect. No significant body weight loss of mice was observed during the treatment in either single or combination drug treatment group (Fig. 4D).

B3 alters multiple biological processes involved in different biologic behaviors of 22Rv1 cells

We performed gene profiling experiments on 22Rv1 cells with KDM4B knocked down or treated with B3 to identify on targets (KDM4B regulated genes) and off targets (non-KDM4B regulated genes) of B3 (Fig. 5A). KDM4B KD resulted in 5281 differentially expressed genes (2189 up and 3092 down, 1.3x change with *padj*<0.05) whereas B3 treatment resulted in 5517 differentially expressed genes (3026 up and 2545 down) (Fig. 5B). 2105 genes (24.1%) were found in both KDM4B KD and B3-treated samples (Fig. 5C). Gene ontology (GO) analysis of common genes indicated several biological processes that were identified previously and involved in KDM4B-promoted tumorigenesis, including cell cycle, mRNA splicing machinery (mRNA process), and EMT (lineage transdifferentiation), which are considered as on-target effect of B3. GO analysis also revealed additional downregulated genes involved in neurogenesis including POU3F2, SOX4, MYC, and WINT5A that are implicated in NEPC in either KDM4B KD or B3 treated samples. Biological processes regulated by the mTOR signaling pathway (translation initiation and elongation) were found to be affected in KDM4B KD or B3 treated cells as well. Unique molecular processes found only in KDM4B KD sample or B3-treated sample included chromatin organization and regulation of cell death, respectively. Differential expression of representative genes involved in aforementioned biological processes were confirmed by qRT-PCR in independent samples (Fig. 5D).

Inhibition of both KDM4B and KDM6A/6B induces cell apoptosis

B3 also targeted genes that were not affected by KDM4B KD, i.e., cell death related gene GADD45A (Fig. 5D). This promoted us to test whether B3 can target other KDMs. Western blot analysis indicated that global H3K9me3 and H3m27me3 but not H3K4me3 were upregulated in B3 treated 22Rv1 cells, suggesting that B3 inhibited both H3K9me3 and H3K27me3 demethylase activities (Fig. 6A). This is further confirmed by demethylase activity assay with 22Rv1 cell lysates treated with vehicle or B3 for 24 hrs (Fig. 6B); B3 inhibited H3K9me3 demethylase activities in a dose-dependent manner. The effect of B3 on H3K27me3 demethylase activities appeared to be lagging behind its effect on H3K9me3 demethylase activities (Fig. 6A). Consistently, we also observed much less inhibition of B3 on H3K27me3 demethylase activities in the demethylase activity assays (Fig. 6B). Both KDM6A and KDM6B are H3K27me3 demethylases and expressed in 22Rv1 cells. B3 inhibited KDM6B with IC_{50} better/similar to that of KDM4B in vitro (Fig. 6C). Combined knockdown of both KDM4B and KDM6A/B resulted in cell apoptosis determined by cleaved PARP1 levels, suggesting the synergistic effect of KDM4B and KDM6A/B (Fig. 6D).

B3 induces tumor cell death and delays DNA damage repair in combination with the mTOR inhibitor rapamycin

The mTOR signaling pathway plays a critical role in cell survival and proliferation and is often upregulated in cancer cells including CRPC. We also observed upregulation of the mTOR signaling in 22Rv1 cells compared to LNCaP cells (Fig. 7A). KDM4B KD in 22Rv1 cells downregulated mTOR signaling under androgen-deprived condition (CFBS+enza) (Fig. 7B). Many genes involved in the mTOR signaling were dysregulated in KDM4B siRNA and/or B3 treated cells (Fig. 5D), suggesting KDM4B may be involved in the mTOR signaling pathway. We tested whether B3 and the mTOR inhibitor rapamycin can synergistically inhibit 22Rv1 cell growth. Addition of rapamycin in B3-treated 22Rv1 cells shifted the growth inhibition curve towards the left with decreased IC_{50} and CI of 0.2 (Fig. 7C), suggesting that B3 and rapamycin has a synergistic effect on growth inhibition of 22Rv1 cells. gH2AX is a marker for stalled DNA replication folks and DNA damage (31). Treatment of double thymidine-synchronized 22Rv1 cells with B3 and rapamycin upregulated gH2AX significantly compared to either B3 or rapamycin alone (Fig. 7D, lane 9 vs lanes 6 & 12). Combined use of B3 and rapamycin also resulted in more cell death compared to either B3 or rapamycin alone (Fig. 7E & F).

B3 synergizes with rapamycin to inhibit 22Rv2 tumor growth

We further tested the effect of combination therapy of B3 plus rapamycin on 22Rv1 xenograft in vivo (Fig. 8). Using low dose of each agent, the combination therapy exhibited the synergistic inhibitory effect on tumor growth. Most importantly, combination therapy also resulted in tumor cell apoptosis as assayed by apoptosis marker, cleaved PARP1 (Fig. 8E).

Discussion

Previously, we found that KDM4B plays an important role in prostate tumorigenesis and suggested that KDM4B may promote PCa progression via promoting alternative splicing of AR gene to generate AR-V7 under castration conditions (28). Here we provide additional evidence supporting this mechanism and furthermore we demonstrated the anti-tumor efficacy of KDM4 inhibitor B3 alone or in combination with enzalutamide or rapamycin. KDM4B overexpression in androgen responsive LNCaP cells promoted tumor growth in vivo (Fig. 1) whereas inactivation of KDM4B in CRPC 22Rv1 cells inhibited tumor growth (Fig. 2). Previously, we found that KDM4B overexpression upregulated AR-V7 expression and promoted resistance of LNCaP cells to anti-androgen drugs that can be mitigated by AR-V7 KD. KDM4B KD in 22Rv1 cells downregulated cell growth and AR-V7 expression and sensitized 22Rv1 cells to enzalutamide, which can be reversed by re-expression of AR-V7 (26). In this study, we showed that downregulation of KDM4B KD 22Rv1 tumor growth in castrated mice can be partially reversed by re-expression of AR-V7 (Fig. 2H). In addition, we showed that KDM4B may promote EMT via AR-V7 (Fig. 2C). Taken together, our data provided strong evidence that KDM4B can promote t-CRPC via AR-V7 and suggested that KDM4B may be an oncogenic factor that promotes CRPC progression. That being said, it is noted that the elevated KDM4B in LNCaP cells failed to increase the tumor-take rate in castrated animals (data not

shown), suggesting that KDM4B alone, although necessary, is not sufficient to account for androgen-independent progression. This could be consistent with the multiple-hits theory of cancer progression as there may be many factors required for CRPC progression in vivo.

Here we evaluated the efficacy of B3 in growth inhibition of 22Rv1 and VCaP xenograft in castrated mice (Fig. 3). B3 demonstrated a superior efficacy in suppressing 22Rv1 tumor growth with large therapeutic window ranging from 1 mg/kg (Fig. 8) to 50 mg/kg (Fig. 3). B3 also sensitized 22Rv1 cells to enzalutamide inhibition in vitro and synergistically inhibited 22Rv1 xenograft growth with enzalutamide (Fig. 4). This data further supports that KDM4B promotes the appearance of t-CPRC by increasing AR-V7 expression, which offers a therapeutic target for t-CRPC patients with high AR-V7 expression. It will be worthy in the future to test this combination in additional preclinical PCa model(s) with high AR-V7 or other AR-variants.

B3 targeted ~40% of KDM4B-regulated genes (2105 out of 5281). KDM4B is a multi-domain protein and can promote gene transcription in a manner dependent or independent of its demethylase activity. The 60% of genes uniquely regulated by KDM4B siRNA and not by B3 are likely those independent of its demethylase activity. There are ~ 62% of genes targeted by B3 and not by KDM4B KD (3466 out of 5571) likely include those regulated by KDMs other than KDM4 such as KDM6 that demethylases H3K27me3/2 as we have shown that B3 inhibited H3K27me3 demethylases (Fig. 6). While these genes in 22Rv1 cells remain to be determined, our data suggests that they may be involved in cell apoptosis as KDM6A/B KD resulted in cell apoptosis that can be further upregulated when combined with KDM4B KD (Fig. 6D).

The synergistic anti-tumor efficacy of B3 and mTOR inhibitor rapamycin is novel and has significant clinical implications. Use of B3 in combination with current PCa targeted therapy may have the potential to increase therapeutic effectiveness and drug safety. The PI3K/Akt/mTOR signaling is elevated in a high proportion of PCa patients and is associated with CRPC progression. Accordingly, PI3K/Akt/mTOR pathway inhibitors are currently being explored as therapeutic agents against hormone sensitive PCa and CRPC. However, the clinical outcome of drugs targeting the PI3K/mTOR signaling pathway as monotherapy in PCa has been thus far disappointing. Inhibition of mTORC1 can result in negative feedback loop of IGF-1R/PI3K-Akt which paradoxically promotes cell survival. The dual mTORC1/2 inhibitor MLN0128 has been tested in patients with metastatic CRPC in phase II clinical trial and showed only limited efficacy, possibly due to the dose reduction secondary to toxicity (32). Our studies suggest that better therapeutic efficacy may be achieved with lower dose of the mTOR inhibitor when used in combination with B3.

The mechanisms underlying the synergy between B3 and rapamycin remains elusive. H3K9me3 are dynamically regulated during cell cycle with relatively low expression during G1/S phase and high in G2/M phase (33). Pharmacological inhibition of H3K9me3 demethylase activity or deletion of KDM4A in squamous cell carcinoma has been shown to induce replication stress and consequent DNA damage in H3K9me3 associated heterochromatin (34). We have also shown previously that KDM4B promotes the expression of PLK1 as co-activator of BMYB. Inhibition of KDM4B by B3 blocked PLK1 expression and

delayed cell cycle progression (27). B3 and KDM4B KD also downregulated the expression of PLK1 and other cell cycle genes such as CCNB1 in 22Rv1 cells (Fig. 5D). mTORC1/2 can enact DNA damage repair and cell survival, resulting in increased cancer cell survival during DNA damage in cancer cells (35). mTORC1 has been shown to promote G2/M checkpoint recovery after DNA damage. Inhibition of mTOCR1 pathways delays mitotic entry after DNA damage through KDM4B-mediated mechanism (36) and sensitize cancer cells to genotoxic DNA damage (35). We speculate that the synergy between B3 and rapamycin may be due to their role in promoting DNA replication stress and/or DNA damage. Consistently, B3 upregulated the expression of gH2A.X in synchronized 22Rv1 cells compared to vehicle control (Fig. 7D). Inhibition of the mTOR signaling by rapamycin under baseline condition had little effect on gH2A.X level but significantly enhanced the effect of B3 on gH2A.X level. B3 could induce DNA replication stress and/or DNA damage at G1. Rapamycin could block the G2/M check point recovery after B3-induced DNA replication stress/damage, thus synergistically arrect cell cycle at G2/M and trigger cell apoptosis.

Conclusion

We have provided experimental evidence that KDM4B is a potent therapeutic target for t-CRPC and B3 is a potential agent with promising therapeutic index. Our data indicated that B3 can be used as a monotherapy or in combination with current anti-PCa regimens and provided scientific rational for future use of epigenetic therapy for PCa.

Abbreviations

AR: Androgen receptor; ARPI: androgen receptor pathway inhibitor; CRPC: castration-resistant prostate cancer; CFBS: charcoal stripped FBS; EMT: epithelial-to-mesenchymal transition; FBS: fetal bovine serum; KD: knockdown; KDM: histone lysine demethylase; NEPC: neuroendocrine prostate cancer; PCa: Prostate cancer.

Declarations

Ethics approval and consent to participate.

All animal protocols were approved by the Institutional Animal Care and Use Committee in UT Southwestern Medical Center. Fresh prostate tumor was obtained with informed consent from a 68 years-old man with Gleason 9 metastatic PCa undergoing radical prostatectomy at the first affiliated hospital of Sun-Yat-San university. Histological sections of prostate biopsy tissue samples were from patients with consent from the First Affiliated Hospital of Sun Yat-sen University, Jiangmen Hospital of Sun Yat-sen University and Affiliated Yantai Yuhuangding Hospital of Qingdao University Medical College from January 2000 to December 2010.

Availability of data and material

All data and materials in this paper are available upon request.

Competing interests

ZPL and EAM are co-founders of Raphael Pharmaceuticals LLC.

Funding

This work is supported in part by grants from the National Key R&D Program of China (2016YFC0902602) and the National Natural Science Foundation of China to J.H.L (81725016) and to Z.H.C. (81902576), NIH RO1HL109471, CPRIT-MIRA RP120717-P1, and DOD PC150152 to Z.P.L., CPRIT-MIRA RP120717-AC and DOD PC150152P2 to J.T.H., NIH R01CA215063 to Z.P.L., J.T.H., and J.-M.A., CPRIT-MIRA RP120717-P4 to J.-M.A., The Welch Foundation (I-1878 to E.D.M) and CPRIT-RP150596 to Bioinformatics Core Facility at UT Southwestern Medical Center.

Authors' contributions

LLD, YAC, YPL performed all the experiments. ZHC, JL, YF, JC, JL, HZ, and JH L designed and performed IHC assays, statistical and survival analysis. YAC, RCP, EH, and JTH designed and performed xenograft tumor studies. TAT and EDM measured demethylase activity and gave intellectual input. PK analyzed tumor pathology. TS and JMA synthesized KDM4B inhibitors. JHL and ZPL designed the study and wrote paper. All authors read and approved the final manuscript.

References

1. Siegel RL, Miller KD, Fuchs HE, Jemal A. Cancer Statistics, 2021. *CA Cancer J Clin* 2021;**71**(1):7-33 doi 10.3322/caac.21654.
2. Lu C, Brown LC, Antonarakis ES, Armstrong AJ, Luo J. Androgen receptor variant-driven prostate cancer II: advances in laboratory investigations. *Prostate Cancer Prostatic Dis* 2020;**23**(3):381-97 doi 10.1038/s41391-020-0217-3.
3. Brown LC, Lu C, Antonarakis ES, Luo J, Armstrong AJ. Androgen receptor variant-driven prostate cancer II: advances in clinical investigation. *Prostate Cancer Prostatic Dis* 2020;**23**(3):367-80 doi 10.1038/s41391-020-0215-5.
4. Tietz KT, Dehm SM. Androgen receptor variants: RNA-based mechanisms and therapeutic targets. *Hum Mol Genet* 2020 doi 10.1093/hmg/ddaa089.
5. Wach S, Taubert H, Cronauer M. Role of androgen receptor splice variants, their clinical relevance and treatment options. *World J Urol* 2020;**38**(3):647-56 doi 10.1007/s00345-018-02619-0.
6. Luo J, Attard G, Balk SP, Bevan C, Burnstein K, Cato L*, et al.* Role of Androgen Receptor Variants in Prostate Cancer: Report from the 2017 Mission Androgen Receptor Variants Meeting. *Eur Urol* 2018;**73**(5):715-23 doi 10.1016/j.eururo.2017.11.038.

7. Sharp A, Coleman I, Yuan W, Sprenger C, Dolling D, Rodrigues DN*, et al.* Androgen receptor splice variant-7 expression emerges with castration resistance in prostate cancer. *J Clin Invest* 2019;**129**(1):192-208 doi 10.1172/JCI122819.
8. Zhang T, Karsh LI, Nissenblatt MJ, Canfield SE. Androgen Receptor Splice Variant, AR-V7, as a Biomarker of Resistance to Androgen Axis-Targeted Therapies in Advanced Prostate Cancer. *Clin Genitourin Cancer* 2020;**18**(1):1-10 doi 10.1016/j.clgc.2019.09.015.
9. Shao C, Yu B, Liu Y. Androgen receptor splicing variant 7: Beyond being a constitutively active variant. *Life Sci* 2019;**234**:116768 doi 10.1016/j.lfs.2019.116768.
10. Clark E, Morton M, Sharma S, Fisher H, Howel D, Walker J*, et al.* Prostate cancer androgen receptor splice variant 7 biomarker study - a multicentre randomised feasibility trial of biomarker-guided personalised treatment in patients with advanced prostate cancer (the VARIANT trial) study protocol. *BMJ Open* 2019;**9**(12):e034708 doi 10.1136/bmjopen-2019-034708.
11. Chen R, Dong X, Gleave M. Molecular model for neuroendocrine prostate cancer progression. *BJU Int* 2018 doi 10.1111/bju.14207.
12. Davies AH, Beltran H, Zoubeidi A. Cellular plasticity and the neuroendocrine phenotype in prostate cancer. *Nat Rev Urol* 2018;**15**(5):271-86 doi 10.1038/nrurol.2018.22.
13. Conteduca V, Oromendia C, Eng KW, Bareja R, Sigouros M, Molina A*, et al.* Clinical features of neuroendocrine prostate cancer. *Eur J Cancer* 2019;**121**:7-18 doi 10.1016/j.ejca.2019.08.011.
14. Nebbioso A, Tambaro FP, Dell'Aversana C, Altucci L. Cancer epigenetics: Moving forward. *PLoS Genet* 2018;**14**(6):e1007362 doi 10.1371/journal.pgen.1007362.
15. Shin S, Janknecht R. Diversity within the JMJD2 histone demethylase family. *Biochem Biophys Res Commun* 2007;**353**(4):973-7 doi 10.1016/j.bbrc.2006.12.147.
16. Fodor BD, Kubicek S, Yonezawa M, O'Sullivan RJ, Sengupta R, Perez-Burgos L*, et al.* Jmjd2b antagonizes H3K9 trimethylation at pericentric heterochromatin in mammalian cells. *Genes Dev* 2006;**20**(12):1557-62 doi 10.1101/gad.388206.
17. Coffey K, Rogerson L, Ryan-Munden C, Alkharaif D, Stockley J, Heer R*, et al.* The lysine demethylase, KDM4B, is a key molecule in androgen receptor signalling and turnover. *Nucleic Acids Res* 2013;**41**(8):4433-46 doi 10.1093/nar/gkt106.
18. Young LC, Hendzel MJ. The oncogenic potential of Jumonji D2 (JMJD2/KDM4) histone demethylase overexpression. *Biochem Cell Biol* 2013;**91**(6):369-77 doi 10.1139/bcb-2012-0054.
19. Kawazu M, Saso K, Tong KI, McQuire T, Goto K, Son DO*, et al.* Histone demethylase JMJD2B functions as a co-factor of estrogen receptor in breast cancer proliferation and mammary gland development. *PLoS One* 2011;**6**(3):e17830 doi 10.1371/journal.pone.0017830.
20. Li W, Zhao L, Zang W, Liu Z, Chen L, Liu T*, et al.* Histone demethylase JMJD2B is required for tumor cell proliferation and survival and is overexpressed in gastric cancer. *Biochem Biophys Res Commun* 2011;**416**(3-4):372-8 doi 10.1016/j.bbrc.2011.11.045.
21. Shi L, Sun L, Li Q, Liang J, Yu W, Yi X*, et al.* Histone demethylase JMJD2B coordinates H3K4/H3K9 methylation and promotes hormonally responsive breast carcinogenesis. *Proc Natl Acad Sci U S A*

2011;**108**(18):7541-6 doi 10.1073/pnas.1017374108.

22. Young LC, McDonald DW, Hendzel MJ. Kdm4b histone demethylase is a DNA damage response protein and confers a survival advantage following gamma-irradiation. *J Biol Chem* 2013;**288**(29):21376-88 doi 10.1074/jbc.M113.491514.
23. Bur H, Haapasaari KM, Turpeenniemi-Hujanen T, Kuittinen O, Auvinen P, Marin K*, et al.* Strong KDM4B and KDM4D Expression Associates with Radioresistance and Aggressive Phenotype in Classical Hodgkin Lymphoma. *Anticancer Res* 2016;**36**(9):4677-83 doi 10.21873/anticanres.11020.
24. Li S, Wu L, Wang Q, Li Y, Wang X. KDM4B promotes epithelial-mesenchymal transition through up-regulation of ZEB1 in pancreatic cancer. *Acta Biochim Biophys Sin (Shanghai)* 2015;**47**(12):997-1004 doi 10.1093/abbs/gmv107.
25. Yang J, AlTahan AM, Hu D, Wang Y, Cheng PH, Morton CL*, et al.* The role of histone demethylase KDM4B in Myc signaling in neuroblastoma. *J Natl Cancer Inst* 2015;**107**(6):djv080 doi 10.1093/jnci/djv080.
26. Duan L, Chen Z, Lu J, Liang Y, Wang M, Roggero CM*, et al.* Histone lysine demethylase KDM4B regulates the alternative splicing of the androgen receptor in response to androgen deprivation. *Nucleic Acids Res* 2019 doi 10.1093/nar/gkz1004.
27. Duan L, Rai G, Roggero C, Zhang QJ, Wei Q, Ma SH*, et al.* KDM4/JMJD2 Histone Demethylase Inhibitors Block Prostate Tumor Growth by Suppressing the Expression of AR and BMYB-Regulated Genes. *Chem Biol* 2015;**22**(9):1185-96 doi 10.1016/j.chembiol.2015.08.007.
28. Duan L, Chen Z, Lu J, Liang Y, Wang M, Roggero CM*, et al.* Histone lysine demethylase KDM4B regulates the alternative splicing of the androgen receptor in response to androgen deprivation. *Nucleic Acids Res* 2019;**47**(22):11623-36 doi 10.1093/nar/gkz1004.
29. Mali P, Yang L, Esvelt KM, Aach J, Guell M, DiCarlo JE*, et al.* RNA-guided human genome engineering via Cas9. *Science* 2013;**339**(6121):823-6 doi 10.1126/science.1232033.
30. Kong D, Sethi S, Li Y, Chen W, Sakr WA, Heath E*, et al.* Androgen receptor splice variants contribute to prostate cancer aggressiveness through induction of EMT and expression of stem cell marker genes. *Prostate* 2015;**75**(2):161-74 doi 10.1002/pros.22901.
31. Turinetto V, Giachino C. Multiple facets of histone variant H2AX: a DNA double-strand-break marker with several biological functions. *Nucleic Acids Res* 2015;**43**(5):2489-98 doi 10.1093/nar/gkv061.
32. Graham L, Banda K, Torres A, Carver BS, Chen Y, Pisano K*, et al.* A phase II study of the dual mTOR inhibitor MLN0128 in patients with metastatic castration resistant prostate cancer. *Invest New Drugs* 2018;**36**(3):458-67 doi 10.1007/s10637-018-0578-9.
33. Hublitz P, Albert M, Peters AH. Mechanisms of transcriptional repression by histone lysine methylation. *Int J Dev Biol* 2009;**53**(2-3):335-54 doi 10.1387/ijdb.082717ph.
34. Zhang W, Liu W, Jia L, Chen D, Chang I, Lake M*, et al.* Targeting KDM4A epigenetically activates tumor-cell-intrinsic immunity by inducing DNA replication stress. *Mol Cell* 2021;**81**(10):2148-65 e9 doi 10.1016/j.molcel.2021.02.038.

35. Silvera D, Ernlund A, Arju R, Connolly E, Volta V, Wang J*, et al.* mTORC1 and -2 Coordinate Transcriptional and Translational Reprogramming in Resistance to DNA Damage and Replicative Stress in Breast Cancer Cells. *Mol Cell Biol* 2017;**37**(5) doi 10.1128/MCB.00577-16.
36. Hsieh HJ, Zhang W, Lin SH, Yang WH, Wang JZ, Shen J*, et al.* Systems biology approach reveals a link between mTORC1 and G2/M DNA damage checkpoint recovery. *Nat Commun* 2018;**9**(1):3982 doi 10.1038/s41467-018-05639-x.

Figures

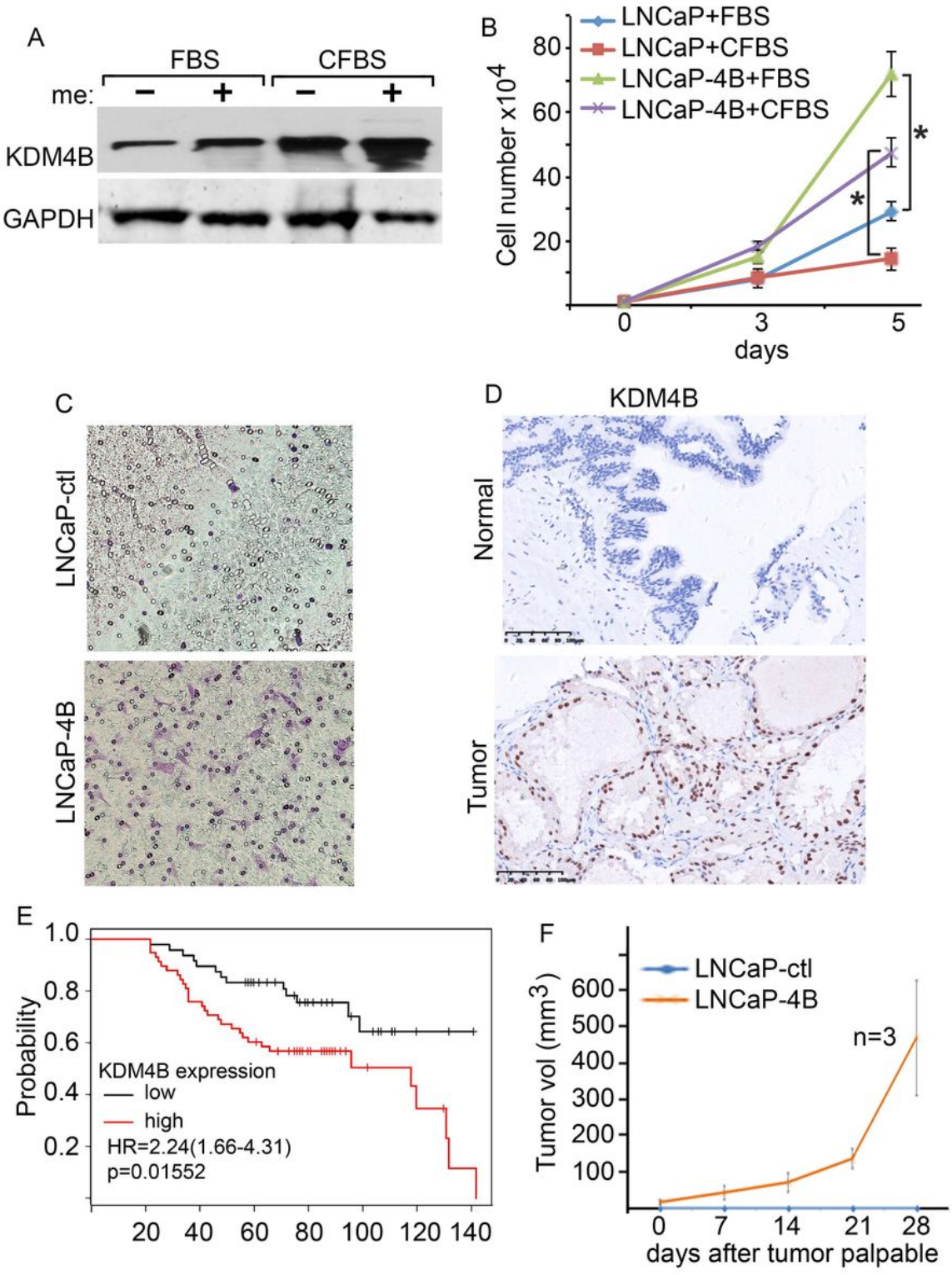

Figure 1

KDM4B promotes prostate tumorigenicity. (A) KDM4B expression in LNCaP cells cultured without (-) or with methylcellulose (me) in the presence of FBS or Charcoal stripped FBS (CFBS). (B) Growth curves of LNCaP-ctl and LNCaP-4B cells in FBS or CFBS (n=5, mean ± SEM). *, p<0.05. (C) Transwell assay showing that LNCaP-4B cells (stained with hematoxylin, in blue) are significantly more migratory than LNCaP-ctl cells. (D) IHC staining of KDM4B (brown) in prostate adenocarcinoma and normal tissues. (E)

Kaplan–Meier overall survival analysis of the correlation between patients with low KDM4B expression (n=48) and high KDM4B expression (n=58) in (D). (F) Growth curves of xenografts derived from LNCaP-4B and LNCaP-ctl cells. mean ± SD. 10 tumors/group. 30% tumor take-up rate was observed in LNCaP-4B cells whereas no tumor was seen in LNCaP-ctl cells.

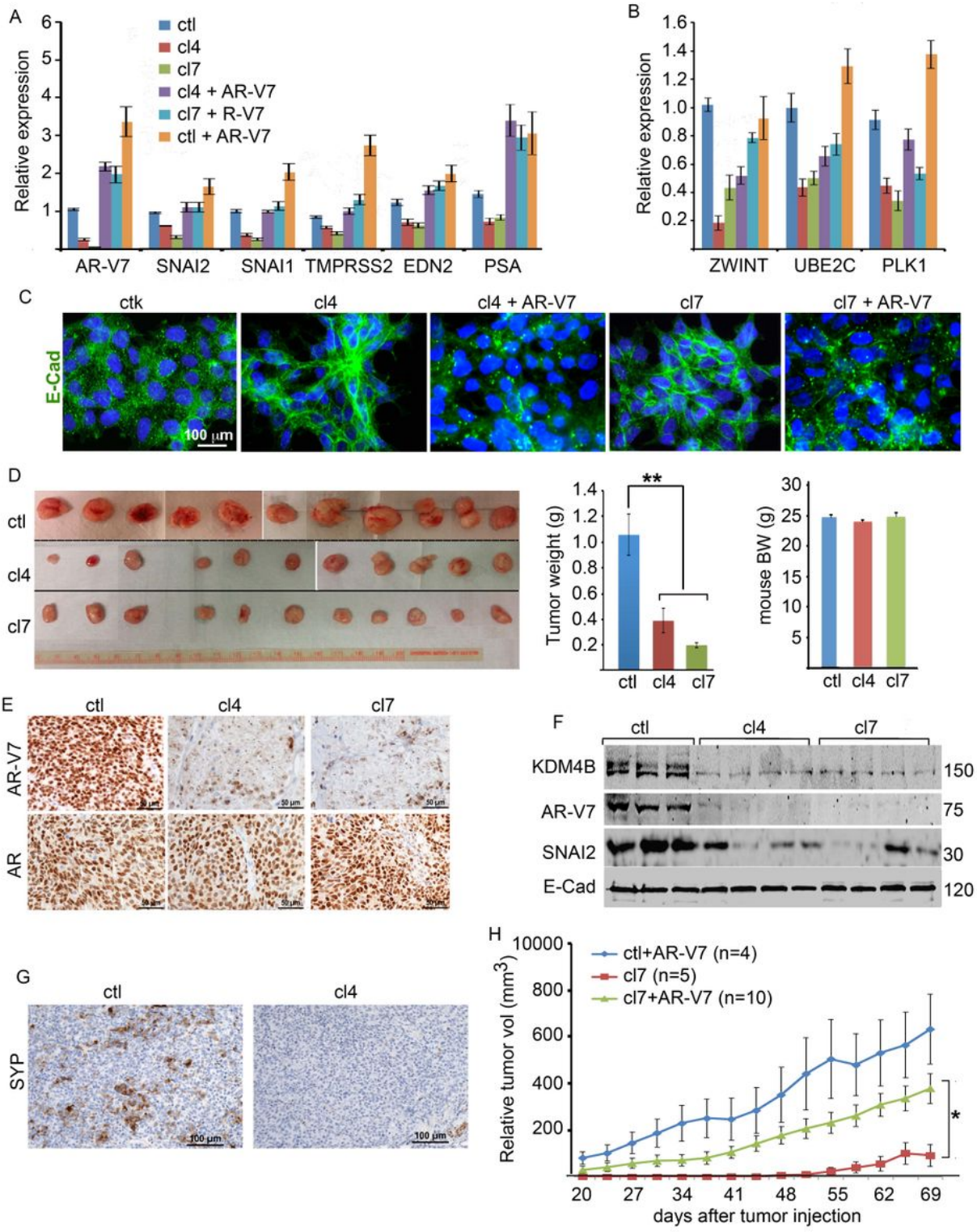

Figure 2

KDM4B knockdown downregulates CRPC growth. 22Rv1 cells were transfected with non-targeting or KDM4B-targeting gRNA. Clonal controls (ctl) and KDM4B KD (cl4, cl7) cells were selected. (A-B) Relative mRNA of genes indicated from ctl, cl4, or cl7 cells in the presence or absence of ectopically expressed AR-V7. mRNAs were normalized against internal GAPDH and expressed relative to control cells transfected with empty vector (n=3, mean ± SD). (C) Immunofluorescence micrographs of indicated cells stained with E-cadherin (E-cad, green) and DAPI. (D) Micrographs of tumor derived from ctl, cl4, and cl7 cells (left panel). Tumor weight and mouse body weight (BW) at time of sacrifice were shown in the middle and right panel, respectively (n=11, mean ± SEM **, p<0.01). (E) Representative IHC staining of AR-V7 and AR in tumors of (D). (F) Western blot of indicated proteins from tumors of (D). (G) Representative IHC staining of SYP in 22Rv1-ctl and KDM4B KD cl4 xenografts. (H) Growth curves of tumors derived from 22Rv1-ctl transfected with AR-V7 (ctl+AR-V7), 22Rv1-cl7 (cl7), and 22Rv1-cl7 transfected with AR-V7 (cl7+AR-V7) cells. Mean± SEM, *, p<0.05.

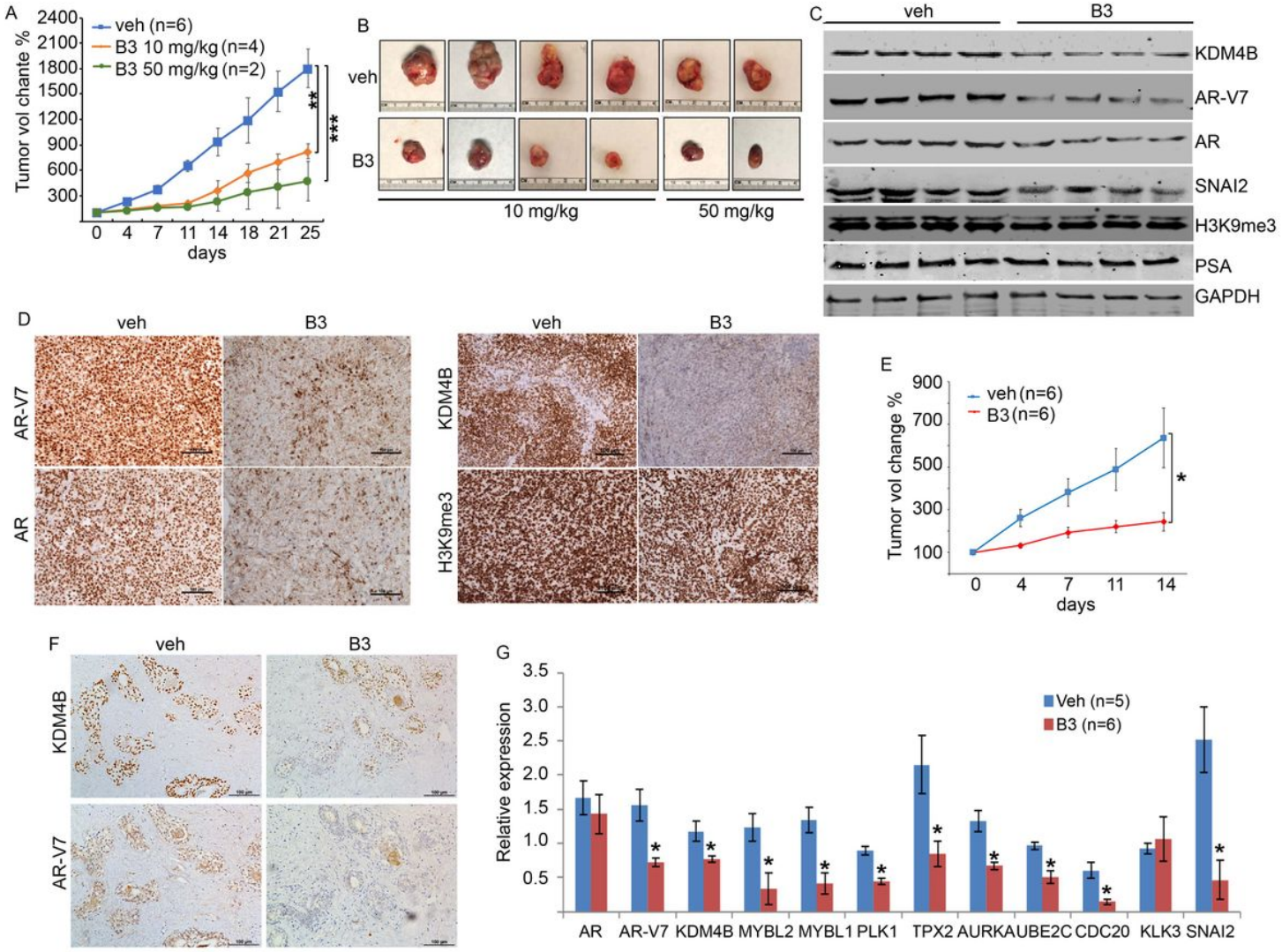

Figure 3

KDM4B inhibitor B3 inhibits the growth of 22Rv1 and VCaP tumors. (A) Growth curves of 22Rv1 xenograft treated with vehicle DMSO (veh) and B3 at 10 mg/kg and 50 mg/kg. Veh or B3 were ip

administered to mice 3 times/week for 2 weeks. Mice were sacrificed 11 days later. (B) Tumor micrographs at time of sacrifice. (C) Western blot of indicated proteins from tumors treated with veh or B3. (D) Representative IHC staining of AR, AR-V7, KDM4B, and H3K9me3 from tumors treated with veh or B3 (50 mg/kg). (E) Grow curves of VCaP xenograft treated with vehicle or B3 (subcutaneous with minipump 50 mg/kg for 7 days). (F) Prostate tumor specimens from a CRPC patient were cultured ex vivo in the presence of vehicle or B3 (2.5μM) for two days. Tissues were fixed and serial sections were IHC-stained with antibodies against KDM4B and AR-V7. (G) Relative mRNA of indicated genes from tumors treated with vehicle or B3 (10mg/kg, ip) (n=3). (A, E, G) Means ± SEM. B3 vs vehicle, *, p<0.05; **, p<0.01, ***, p<0.005.

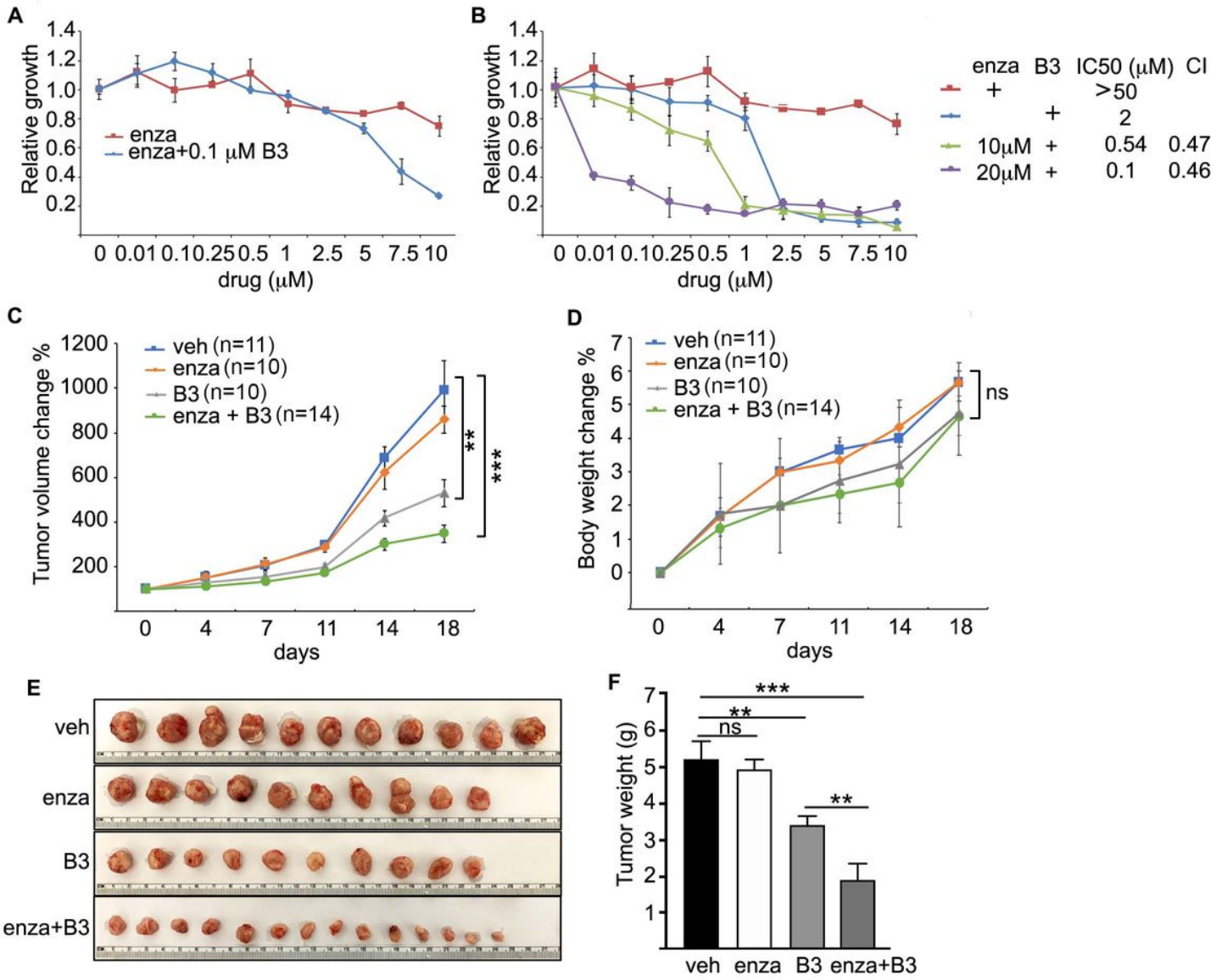

Figure 4

B3 sensitizes 22Rv1 cells to enzalutamide and inhibits castration-resistant tumor growth. (A) Growth curves of 22Rv1 cells in the presence of various concentration of enzalutamide (enza) alone or in the

presence of B3 (0.1 μM) (n=6, mean ± SD). (B) Dose response curves of 22Rv1 cells to B3, enza, or B3+enza as indicated. CI was calculated based on the IC50 of single compound or compounds in combination. (C) Tumor growth curves of 22Rv1-xenografts treated with vehicle (DMSO), enza (20 mg/kg), B3 (5mg/kg), B3+enza. (D) % of mouse body weight change of various treatment groups during the treatment. (E) Micrographs of tumors in indicated treatment groups and (F) Tumor wight at time of sacrifice. Mean ± SEM, **, p<0.01. ***, p<0.005. ns: not significant.

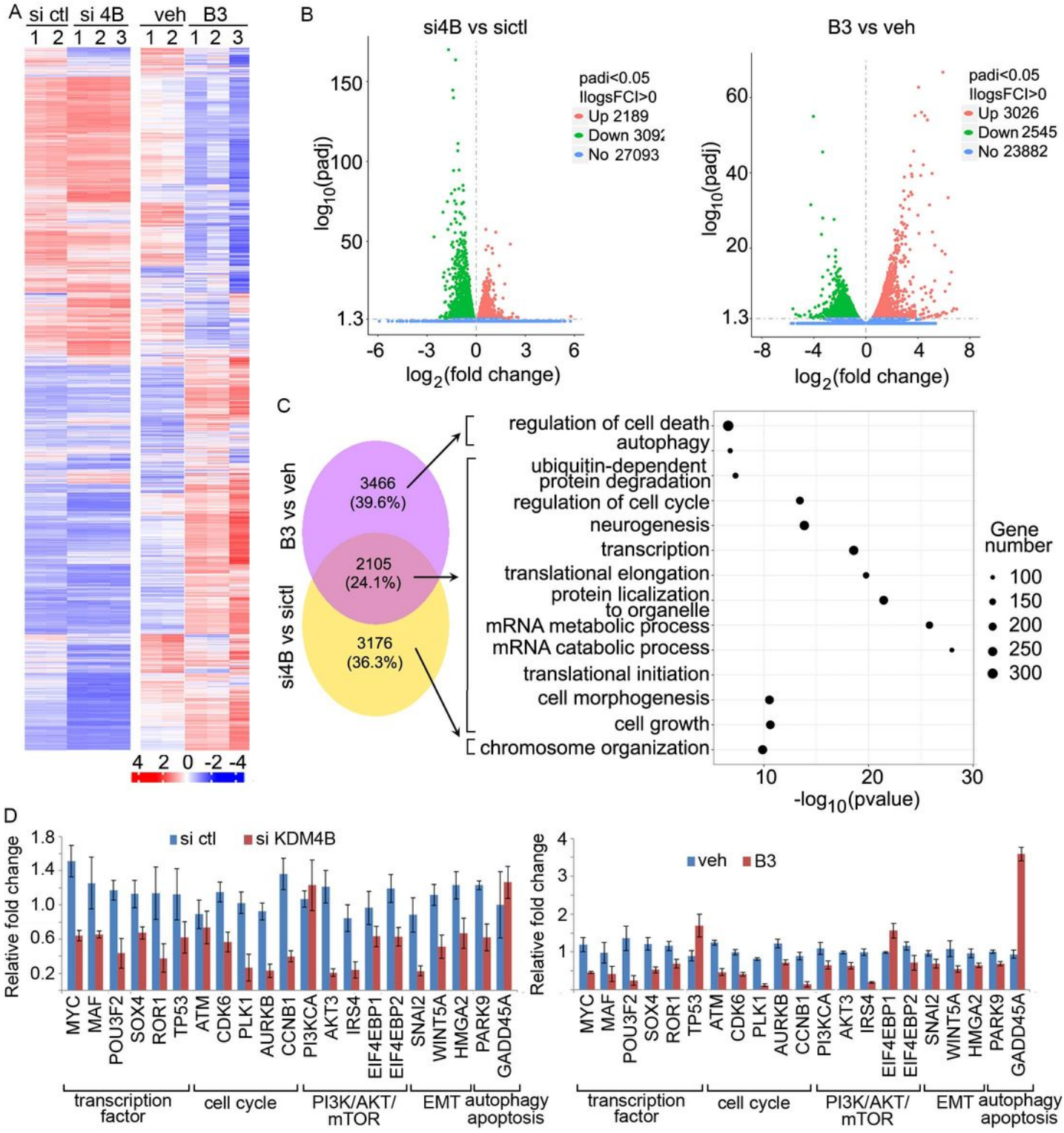

Figure 5

B3 targets multiple biological processes in PCa cells. (A) Heatmaps of differentially expressed genes of 22Rv1 treated with KDM4B siRNA or B3. (B) Volcano plot of differentially expressed genes in 22Rv1 cells transfected with control or KDM4B siRNA (left panel) and in 22Rv1 cells treated with vehicle or B3 (right panel). (C) Venn plot showing unique and common genes associated by KDM4B siRNA and B3 treatment in 22Rv1 cells (left panel). The GO terms associated with unique and common gene sets are shown on the right. (D) Relative mRNA of representative differentially expressed genes in 22Rv1 cells transfected with control vs KDM4B siRNA and in cells treated with vehicle vs B3 (n=3, mean ± SEM).

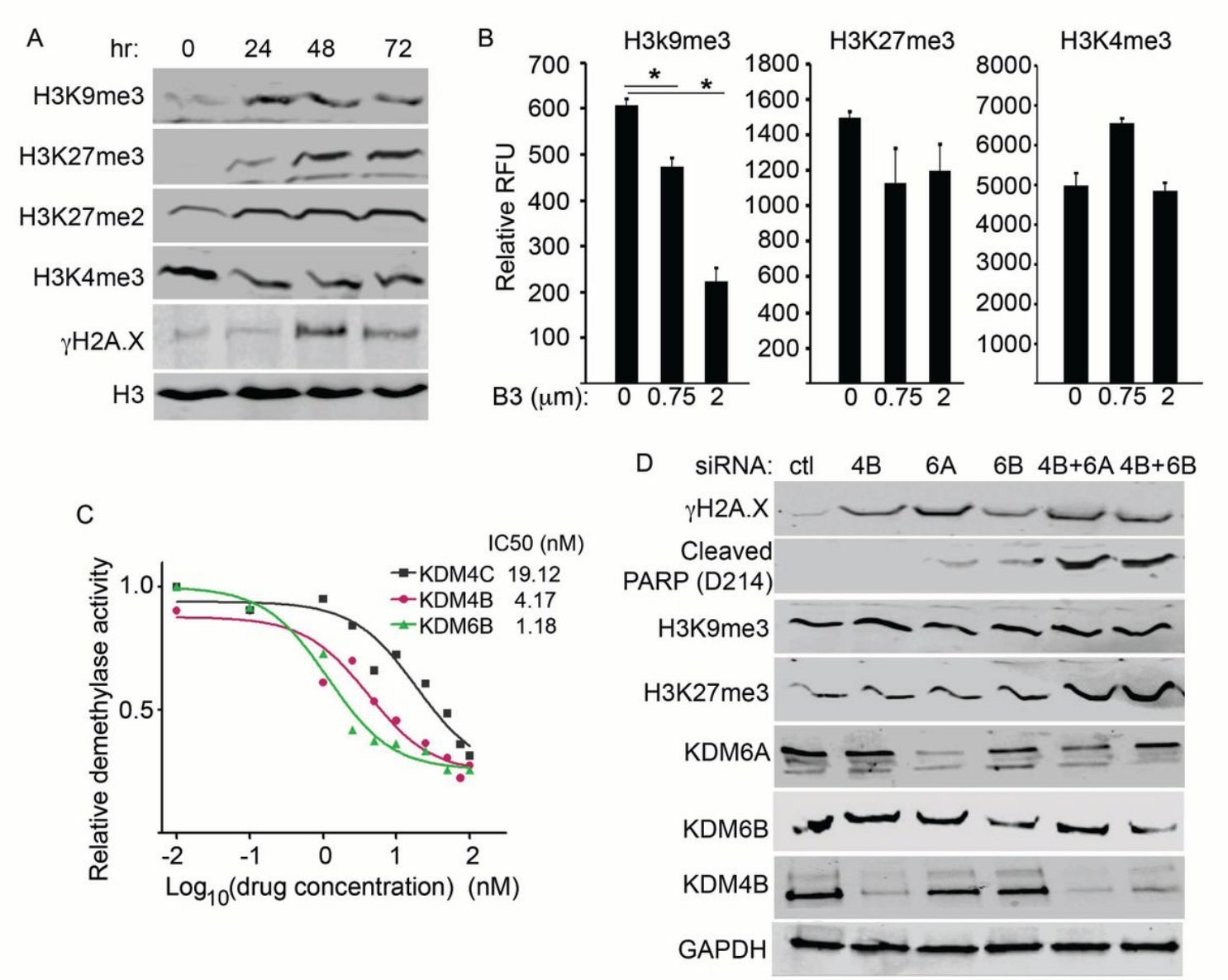

Figure 6

B3 inhibits the activities of H3K9me3 demethylase (KDM4B) and H3K27me3 demethylase (KDM6B). (A) Western blots of methylated histones and γH2A.X in 22Rv1 cells after treatment with B3 for indicated time points. (B) H3K9me3 and H3K27me3 demethylase activities in 22Rv1 cell lysates treated with various concentration of B3 (n=3). (C) Relative demethylase activities of recombinant protein KDM4C, KDM4B, and KDM6B in the presence of various concentration of B3 (n=6). (D) Western blot of indicated

proteins from 22Rv1 cells transfected with control siRNA or siRNA targeting KDM4B, KDM6A, KDM6B, or combination of KDM4B plus KDM6A/B.

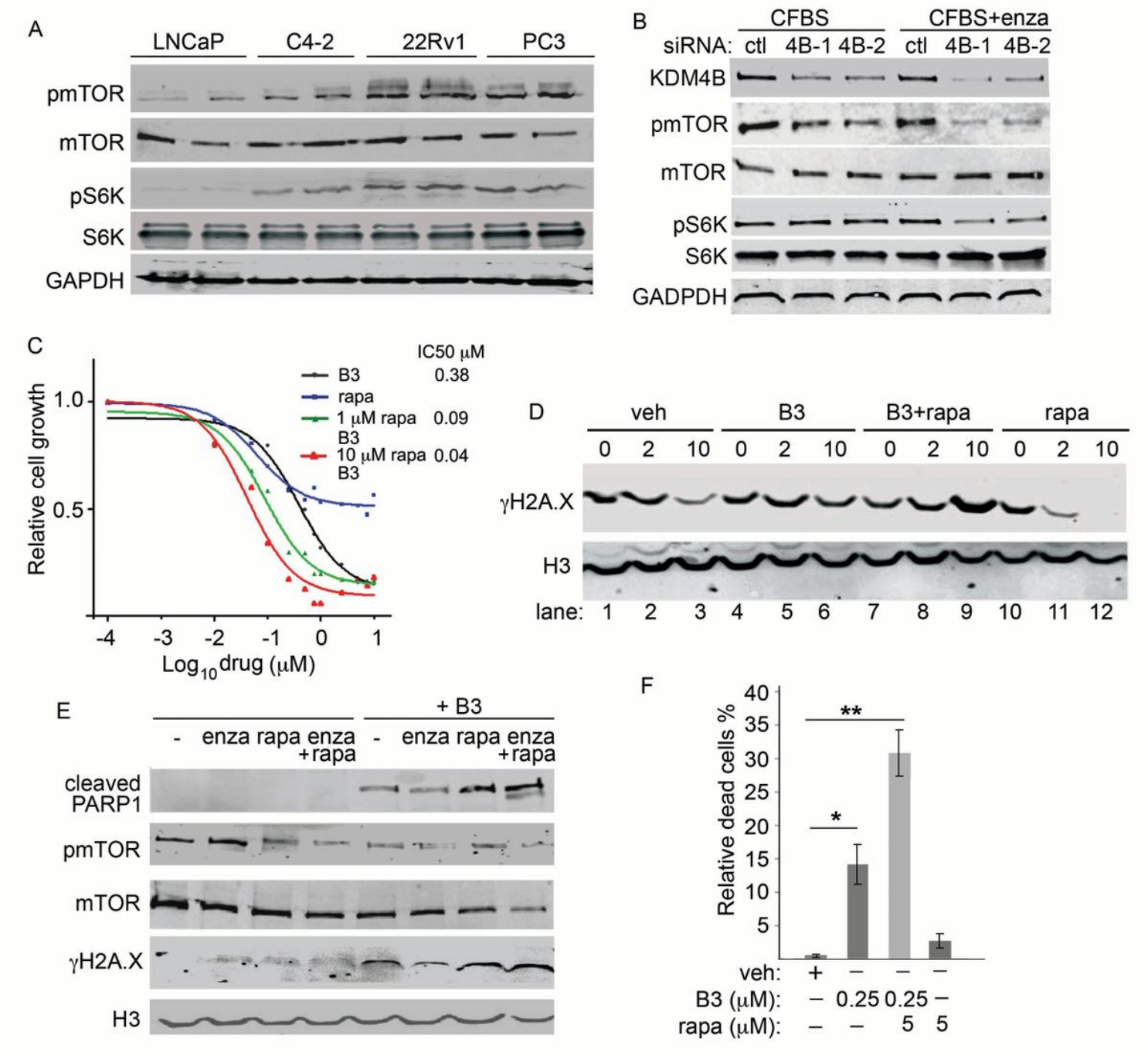

Figure 7

Combination therapy of B3 and rapamycin synergizes tumor cell death. (A) Western blots of proteins involved in the mTOR signaling pathway in various PCa cell lines. (B) Western blots showing the mTOR signaling was downregulated in 22Rv1 cells transfected with two independent KDM4B siRNAs compared to control siRNA transfected cells. (C) Relative growth of 22Rv1 cells treated with various concentrations of B3, rapamycin (rapa), or combination of B3 plus rapamycin. IC50 was calculated using Graphpad. (D) Western blot of γH2A.X at indicated time points in synchronized 22Rv1 cells after releasing from double-thymidine block. H3 was used as the loading control. 22Rv1 cells were treated with B3, rapamycin, or B3

plus rapamycin at time of withdrew thymidine (0 h). (E) Wester blots of indicated proteins from 22Rv1 cell lysates treated with enzalutamide (enza), rapamycin, B3, or combination of the three as indicated. (F) % of dead cells in 22Rv1 cells treated with B3, rapamycin, or B3 plus rapamycin for 52 hrs. n=3, mean ± SEM.

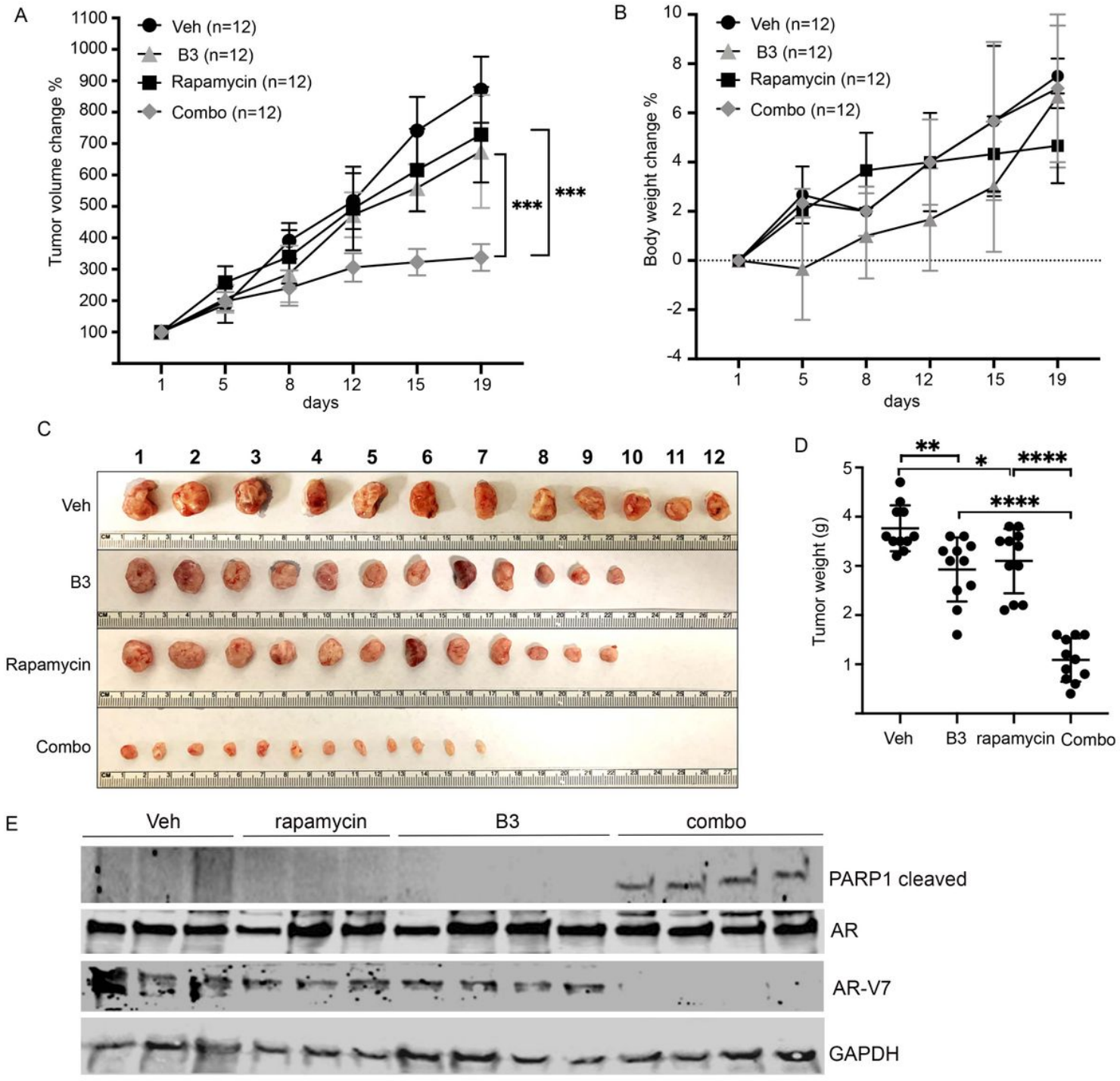

Figure 8

B3 and rapamycin synergistically block 22Rv1 tumor growth. (A) Relative growth curve of 22Rv1 xenograft in castrated mice. Tumor-bearing mice were treated with B3 (1mg/kg), rapamycin (rapa) (2mg/kg), or combination at day 1 for 2 weeks (three times-a-week, ip). Tumors were harvested at day 19.

(B) % body weight change of mice during treatment period. (C) Micrograph of tumors harvested. (D) Tumor weight of various treatment groups. (E) Western blot of indicated proteins from tumor tissues in C.

Supplementary Files

This is a list of supplementary files associated with this preprint. Click to download.

- Supplementalfigtable.pdf